IEEE Access
Multidisciplinary | Rapid Review | Open Access Journal

Received February 28, 2021, accepted March 13, 2021, date of publication March 18, 2021, date of current version March 30, 2021.

Digital Object Identifier 10.1109/ACCESS.2021.3067046

Robust Head-Pursuit Guidance Accounting for Hit-to-Kill and Angle Constraints

FENG YANG, GUANG-QING XIA, AND KAI LIU

State Key Laboratory of Structural Analysis for Industrial Equipment, School of Aeronautics and Astronautics, Dalian University of Technology, Dalian 116024, China

Key Laboratory of Advanced Technology for Aerospace Vehicles of Liaoning Province, School of Aeronautics and Astronautics, Dalian University of Technology, Dalian 116024, China

Corresponding author: Feng Yang (feng_yang@ dlut.edu.cn)

ABSTRACT In this paper, the hit-to-kill strategy is introduced to solve the three-dimensional (3D) robust head-pursuit (HP) interception problem considering the line-of-sight (LOS) angle constraints. Firstly, a target based relative dynamic model is proposed to be the nominal model for designing the robust HP guidance laws, where the HP interception problem is formulated as a target passively chases after the interceptor missile. Secondly, the 3D retro-proportional navigation (RPN) guidance law is reinterpreted from the point of control theory, which forces the corresponding guidance system asymptotically stable. Meanwhile, the concept of nullifying the LOS angular rates is successfully introduced to solve the 3D robust HP guidance problem via the sliding mode control. Thirdly, the LOS angles constrained robust HP guidance law is proposed based on the nonsingular terminal sliding mode control. The stabilities of the presented guidance laws are analyzed via the Lyapunov approach. The simulation results are in agreement with the theoretical statements.

INDEX TERMS Missiles, guidance, head-pursuit interception, retro-proportional navigation, sliding mode control.

I. INTRODUCTION

It is a challenging task to intercept a high-speed target (such as a hypersonic glider) by an interceptor missile, especially when the missile's velocity is inferior to that of the target. One reason for this plight is that the traditional defense missile usually performs the head-on (HO) interception strategy, where the closing velocity is so huge that stringent requirements on the missile guidance system are imposed. Recently, the head-pursuit (HP) interception strategy [1] has been proposed to concern this problem, where the missile is placed such that the target passively chases after the interceptor missile. The so-called HP guidance law [2]–[5] and the retro-proportional navigation (RPN) guidance law [6]–[8] have been proposed to fulfill the HP interception engagement. However, the HP guidance problem has not been adequately studied. At least, the hit-to-kill strategy has not been applied to the HP interception problem. To this end, it is necessary to find new solutions for the robust HP guidance law design, so that a hypersonic maneuvering target can be intercepted within a finite time by a speed inferior interceptor missile.

The associate editor coordinating the review of this manuscript and approving it for publication was Zhenbao Liu.

The so-called HP guidance [2]–[5] is indeed an extended application of the deviated-velocity-pursuit (DVP) method [9] in the HP interception. Compared with the traditional DVP method, the HP DVP method ensures that the lead angles of the interceptor missile keep proportional to the varying lead angles of the target. However, since *the target's lead angles are hard to be measured on-board*, the HP DVP method is difficult to be directly performed by a homing missile. Later, a generalized DVP method that aims to maintain expected lead angles of the interceptor missile is proposed [10], which is known as intercept angle guidance. However, especially when intercepting a maneuvering target, *these DVP based guidance laws easily result in a highly curled trajectory of the interceptor missile*, which is not preferred in practical applications. The RPN guidance method [6]–[8] introduces a more feasible approach for performing HP interception. The 3D RPN guidance law takes the same mathematical form of the pure proportional navigation (PPN) guidance law, except for the counter-intuitive negative navigation constant. Due to the multi-value characteristic of the collision triangle, the RPN approach asymptotically nullifies the line-of-sight (LOS) angular rate so that the interceptor missile kills the target at the far impact point. Though the RPN guidance law almost admits the merits of the PPN method,

the RPN guidance is not robust to the maneuvers of the target.

Since the traditional finite-time robust guidance laws [11]–[15] can be understood as the nonlinear extension of the PN method. The robust HP guidance may be obtained from the results of the RPN method. However, the planar model used in the RPN method restricts the investigation of the general 3D robust HP guidance. Inspired by the disposal process of the impact angle constraint in [16], why do not we formulate the HP interception problem in the target based LOS framework? Refer to [10], the definition of the interceptor-centered HP problem is just in accordance with the definition of the target-centered tail-chase (TC) problem. This idea can be summarized as that *the target passively chases after the interceptor missile*. In such a way, *the relative dynamics turn out to be familiar, where the most difference is that the gain's symbols before the control variables are changed*. Moreover, the necessary guidance information can be directly obtained from the measurements of the homing missile, which will be shown in the next section. Now, the concept of nullifying LOS angular rate may could be applied without losing generality. In another word, the hit-to-kill strategy could be introduced to the HP interception problem.

Furthermore, the LOS angle constrained finite-time robust HP guidance problem can also be addressed based on the new nominal model. In many literature, angle constraints are usually transformed to be the LOS angle constraints, such as field-of-view constrained problems [17], [18] and impact angle constrained problems [19]–[24]. *Due to the axial symmetry property between the missile-based LOS coordinate system and the target-based LOS coordinate system, the LOS angle constraints for the interceptor missile can be easily transformed to be the constraints of the target's LOS angle*. In this paper, the nonsingular terminal sliding mode (NTSM) control [25] will be employed to demonstrates the LOS angle constrained HP guidance law.

The main contributions of this paper are summarized as follows. (1) A new generalized 3D mathematical formulation for the HP interception problem is proposed by formulating the HP problem as a target-based passive TC problem, which greatly simplifies the complexity of the nominal model for the HP problem. (2) The RPN guidance law is represented and analyzed from the point of control theory, where the RPN based guidance system is proven to be asymptotically stable. Subsequently, the SMC based HP guidance law shows that the classical concept of nullifying the LOS angular rate can be utilized to the HP guidance problem. (3) Constrained HP guidance law accounting for LOS angles is firstly proposed based on the NTSM method, which shows another choice for solving the angle constrained robust HP guidance problem.

The paper is organized as follows. In Section II, the new HP guidance design framework is proposed, as well as the access to the necessary guidance information. From the point of control theory, the RPN guidance law is reinterpreted based on the new nominal model in Section III. The SMC-based robust HP guidance law is also proposed in this section.

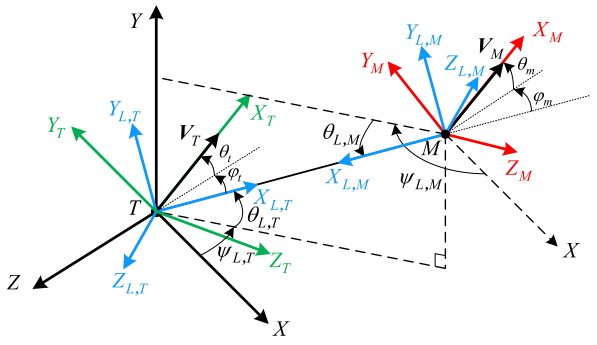

FIGURE 1. Three-dimensional interception geometry.

In Section IV, the LOS angle constrained robust HP guidance law is deduced for intercepting a maneuvering target based on the NTSM method. The numerical simulations and the conclusions of this paper are respectively presented in Section V and Section VI.

II. PROBLEM STATEMETS AND PRELIMINARIES

In this section, the target-centered coupling 3D target-missile engagement dynamics is constructed, the design objective and the preliminaries are presented.

A. TARGET BASED RELATIVE DYNAMICS

The interceptor missile based HP interception engagement is reformulated as a target based TC interception engagement, as shown in Figure 1. The reference frames used in this paper are defined as the inertial frame, the target frame, the interceptor missile frame, and the LOS frame denoted by XYZ, $X_TY_TZ_T$, $X_MY_MZ_M$, and $X_LY_LZ_L$, respectively. The inertial frame is located at the initial location of the target. The LOS frames of the target (LOS-T) and that of the interceptor missile (LOS-M) are distinguished by the additional subscripts, T and M, respectively. Except for definite emphasis, the LOS-T frame is chosen to be the fundamental LOS frame without the subscript T. Moreover, the LOS frame is oriented by the pair of azimuth and elevation angles $\{\psi_L, \theta_L\}$ with respect to the inertial frame.

Both the target and the interceptor missile are assumed to be point masses, and their velocity vectors, denoted by $\boldsymbol{V}_T$ and $\boldsymbol{V}_M$, are aligned with the X axes of their body frame. Moreover, the corresponding speeds of them, V_t and V_m, are constants. The body frames of the target and the interceptor missile are oriented by the pairs of lead angles $\{\psi_t, \theta_t\}$ and $\{\psi_m, \theta_m\}$ to the LOS frame, respectively. Furthermore, the target and the interceptor missile are controlled by their lateral accelerations. The seeker and autopilot dynamics of the missile are fast enough to be neglected. The angle-of- attack is small enough to be neglected. Then, similar to [26], the relative kinematics and dynamics can be obtained as follows.

$$\frac{\mathrm{d}\boldsymbol{r}_L}{\mathrm{d}t} - \boldsymbol{V}_M = \boldsymbol{V}_T = \boldsymbol{V}_L + \frac{\delta \boldsymbol{r}_L}{\delta t.} \times \boldsymbol{\omega}_L \boldsymbol{r}_L \tag{1}$$

$$\frac{\mathrm{d}\boldsymbol{V}_L}{\mathrm{d}t} = \boldsymbol{A}_M - \boldsymbol{A}_T = \frac{\delta \boldsymbol{V}_L}{\delta t} + \boldsymbol{\omega}_L \times \boldsymbol{V}_L \tag{2}$$

$$\boldsymbol{A}_M = a_{ym}\boldsymbol{j}_M + a_{zm}\boldsymbol{k}_M = \boldsymbol{\omega}_L \times \boldsymbol{V}_M + \boldsymbol{\omega}_M \times \boldsymbol{V}_M \tag{3}$$

$$\boldsymbol{A}_T = a_{yt}\boldsymbol{j}_T + a_{zt}\boldsymbol{k}_T = \boldsymbol{\omega}_L \times \boldsymbol{V}_T + \boldsymbol{\omega}_T \times \boldsymbol{V}_T \tag{4}$$

where

$$\begin{aligned}
\boldsymbol{r}_L &= r\boldsymbol{i}_L \\
\boldsymbol{V}_L &= V_r\boldsymbol{i}_L + V_\theta\boldsymbol{j}_L + V_\psi\boldsymbol{k}_L = \dot{r}\boldsymbol{i}_L + r\dot{\theta}_L\boldsymbol{j}_L - r\dot{\psi}_L\cos\theta_L\boldsymbol{k}_L \\
\boldsymbol{\omega}_L &= \dot{\psi}_L\sin\theta_L\boldsymbol{i}_L + \dot{\psi}_L\cos\theta_L\boldsymbol{j}_L + \dot{\theta}_L\boldsymbol{k}_L \\
\boldsymbol{\omega}_M &= \dot{\psi}_m\sin\theta_m\boldsymbol{i}_M + \dot{\psi}_m\cos\theta_m\boldsymbol{j}_M + \dot{\theta}_m\boldsymbol{k}_M
\end{aligned}$$

The rotation angular vector $\boldsymbol{\omega}_T$ can be obtained from the definition of $\boldsymbol{\omega}_M$ by replacing the subscript M (m) by $T(t)$. The relative dynamics (2) can be expanded as

$$\begin{aligned}
\ddot{r} - r\dot{\theta}_L^2 - r\dot{\psi}_L^2\cos^2\theta_L &= a_{xL,M} - a_{xL,T} \\
r\ddot{\theta}_L + 2\dot{r}\dot{\theta}_L + r\dot{\psi}_L^2\sin\theta_L\cos\theta_L &= a_{yL,M} - a_{yL,T} \\
-r\ddot{\psi}_L\cos\theta_L - 2\dot{r}\dot{\psi}_L\cos\theta_L + 2r\dot{\theta}_L\dot{\psi}_L\sin\theta_L & \\
= a_{zL,M} - a_{zL,T} &
\end{aligned} \tag{5}$$

where the right-hand-side variables of (5) are the acceleration projections of the target and the interceptor missile in the LOS frame. The missile's acceleration is expanded as

$$\begin{aligned}
a_{xL,M} &= -\sin\theta_m\cos\psi_m \cdot a_{ym} + \sin\psi_m \cdot a_{zm} \\
a_{yL,M} &= \cos\theta_m \cdot a_{ym} \\
a_{zL,M} &= \sin\theta_m\sin\psi_m \cdot a_{ym} + \cos\psi_m \cdot a_{zm}
\end{aligned} \tag{6}$$

If replacing the subscript $M(m)$ by $T(t)$, then (6) expresses the target's acceleration projections.

For an endo-atmospheric interception engagement, the nonlinear and coupled engagement dynamics, as shown in (5), is more accurate than the traditional decoupled dynamics. Noted that a_{ym} not only effects on the elevation direction but also on the azimuth direction, which should be concerned in guidance law design. Otherwise, the guidance accuracy may be degraded. In addition, some assumptions are given as follows.

Assumption 1: Suppose that the lateral accelerations of the target are uniformly bounded throughout the engagement.

Assumption 2: Suppose that the necessary guidance signals $r, \dot{r}, \theta_{L,M}, \psi_{L,M}, \dot{\theta}_{L,M}, \dot{\psi}_{L,M}, \theta_m$, and ψ_m can be measured by the homing interceptor missile. Furthermore, the lead angles of the interceptor missile and the target strictly belong to the interval $\left(-\pi/2, \pi/2\right)$.

Assumption 3: Suppose that the relative velocity between the interceptor missile and the target is negative throughout the engagement. Considering the physical structure of the vehicles, the impact occurs when the relative range decreases to a reasonable level, i.e. $r(t_f) \le r_{\lim}$.

The Assumption 1 is valid due to the physical limits of an aircraft. Based on Assumption 2, the interceptor missile can obtain all the necessary guidance signals, however, these signals should be processed to match the proposed relative dynamics. Because of the axial symmetric characteristic between LOS-M and LOS-T, the following equations are obviously valid.

$$\theta_L = \theta_{L,T} = -\theta_{L,M}, \quad \psi_L = \psi_{L,T} = \psi_{L,M} + \pi \tag{7}$$

$$\dot{\theta}_L = \dot{\theta}_{L,T} = -\dot{\theta}_{L,M}, \quad \dot{\psi}_L = \dot{\psi}_{L,T} = \dot{\psi}_{L,M} \tag{8}$$

Subsequently, the proposed relative dynamics can be used as the nominal model with sufficient guidance information. The constraints on the lead angles of the interceptor missile and the target guarantee the existence of a strict HP interception engagement. If the assumption is violated, then the traditional guidance method should be recovered. Assumption 3 helps us to ignore the influence of the relative velocity so that the nominal guidance model only concerns the variations of LOS angles. Moreover, this assumption can be guaranteed by choosing the initial parameters of the terminal engagement. And, the impact success condition is decided by the vehicle physical structure.

B. GUIDANCE OBJECTIVES

The first question is *how to realize the hit-to-kill strategy in HP interception engagement*. If the LOS angular rates can be nullified within finite time, then the interceptor missile and the target will come into the impact course. Based on the proposed relative dynamics, the objective of the hit-to-kill HP guidance law design can be stated as follows. There exist $t_c \ge 0$ such that

$$\dot{\theta}_L = 0, \quad \dot{\psi}_L = 0, \quad for\ t_c \le t \le t_f \tag{9}$$

holds, where t_f is the final time moment of the engagement. From (8), it can be seen that the LOS angular rates of the target and the interceptor missile will be nullified at the same time.

As many angle constrained guidance problem can be transformed into the LOS angle constrained guidance problem. The second question is *verifying the effectiveness of the proposed relative dynamics on the LOS angles constrained robust HP guidance problem*. The design objective is summarized as follows. There exist $t_c \ge 0$ such that

$$\begin{aligned}
\theta_L &= \theta_L^*, \quad \psi_L = \psi_L^* \\
\dot{\theta}_L &= 0, \quad \dot{\psi}_L = 0
\end{aligned} \quad for\ t_c \le t \le t_f \tag{10}$$

holds, where θ_L^* and ψ_L^* are the expected elevation and azimuth angles.

Moreover, taking Assumption 3 into account, the first equation in (5) can be ignored. Then, the nominal model can be expressed in a more concise form as follows.

$$\begin{bmatrix} \ddot{\theta}_L \\ \ddot{\psi}_L \end{bmatrix} = \boldsymbol{F} + \boldsymbol{D} + \boldsymbol{B}\boldsymbol{u} \tag{11}$$

where

$$\boldsymbol{F} = \begin{bmatrix} -\frac{2\dot{r}}{r}\dot{\theta}_L - \dot{\psi}_L^2\sin\theta_L\cos\theta_L \\ -\frac{2\dot{r}}{r}\dot{\psi}_L + 2\dot{\theta}_L\dot{\psi}_L\tan\theta_L \end{bmatrix},$$

$$\boldsymbol{D} = \begin{bmatrix} -\frac{\cos\theta_t \cdot a_{yt}}{r} \\ \frac{\sin\theta_t\sin\psi_t \cdot a_{yt} + \cos\psi_t \cdot a_{zt}}{r\cos\theta_L} \end{bmatrix}$$

$$\boldsymbol{B}=\begin{bmatrix}\frac{\cos\theta_m}{r} & 0\\ -\frac{\sin\theta_m\sin\psi_m}{r\cos\theta_L} & -\frac{\cos\psi_m}{r\cos\theta_L}\end{bmatrix},\quad \boldsymbol{u}=\begin{bmatrix}a_{ym}\\ a_{zm}\end{bmatrix}$$

The gain matrix $\boldsymbol{B}$ should be nonsingular during the engagement so that the control input $\boldsymbol{u}$ is effective.

C. PRELIMINARIES

The following notations will be used in this paper. $\mathbf{R}$ the set of real numbers and $\mathbf{R}_+$: $\{x\in\mathbf{R}\,|x>0\}$. For a vector $\boldsymbol{x}\in\mathbf{R}^n$, its norm is defined as $\|\boldsymbol{x}\|\triangleq\sqrt{x_1^2+x_2^2+\cdots+x_n^2}$. The function $\lceil x\rfloor^\alpha$ is a symbol definite function $\lceil x\rfloor^\alpha=|x|^\alpha\,\mathrm{sign}\,(x)$, where sign (x) the signum function, $\alpha\in\mathbf{R}_+\cup\{0\}$ and $x\in\mathbf{R}$. It follows that, $\mathrm{d}\lceil x\rfloor^\alpha/\mathrm{d}t=\alpha\,|x|^{\alpha-1}\dot{x}$. For a vector $\boldsymbol{x}\in\mathbf{R}^n$ and $\alpha\geq 0$, $\lceil\boldsymbol{x}\rfloor^\alpha\triangleq[\lceil x_i\rfloor^\alpha,\cdots,\lceil x_i\rfloor^\alpha,\cdots,\lceil x_n\rfloor^\alpha]^T$.

Lemma 1 [27]: Consider the nonlinear system $\dot{\boldsymbol{x}}=\boldsymbol{f}(\boldsymbol{x},t)$, $\boldsymbol{x}\in\mathbf{R}^n$. Assuming that there exist a continuous and positive definite function $V(\boldsymbol{x})$ satisfies

$$\dot{V}(\boldsymbol{x})\leq-\lambda V^\alpha(\boldsymbol{x}) \tag{12}$$

where $\lambda\in\mathbf{R}_+$, and $0<\alpha<1$ are constants. $\boldsymbol{x}(t_0)=\boldsymbol{x}_0$ the initial states. Then, the system state will converge to the equilibrium within a finite time T.

$$T\leq\frac{V^{1-\alpha}(0)}{\lambda(1-\alpha)} \tag{13}$$

Lemma 2 [28]: For $b_i\in\mathbf{R}$, $i=1,2,\cdots,n$, $0<q<1$, the following inequality holds.

$$(|b_1|+|b_2|+\cdots+|b_n|)^q\leq|b_1|^q+|b_2|^q+\cdots+|b_n|^q \tag{14}$$

III. RPN AND 3D ROBUST HP GUIDANCE LAW

In this section, the RPN guidance law will be represented based on the proposed relative dynamics. The SMC will be used to design the 3D hit-to-kill HP guidance law.

A. RPN GUIDANCE LAW AND LYAPUNOV ANALYSIS

As shown in [26], the on-board seeker usually cannot measure the component of the LOS angular rate along the LOS. Moreover, the spin of the LOS does not affect the moving direction of the LOS [7], [29]. Hence, let us define the key part of the LOS angular rate as follow.

$$\boldsymbol{\omega}_R=\dot{\psi}_L\cos\theta_L\boldsymbol{j}_L+\dot{\theta}_L\boldsymbol{k}_L \tag{15}$$

where $\boldsymbol{\omega}_R=\boldsymbol{\omega}_L-\dot{\psi}_L\sin\theta_L\boldsymbol{i}_L$ decides the moving direction of the LOS. Based on the proposed relative dynamics, the RPN guidance law can be represented as

$$N_R\boldsymbol{\omega}_R\times\boldsymbol{V}_M,\quad N_R<0 \tag{16}$$

where N_R is chosen such that $\exists N>2$ makes the following equality holds.

$$N_R=\frac{N\dot{r}}{V_m\cos\theta_m\cos\psi_m},\quad N>2 \tag{17}$$

The stability of the represented RPN method is concluded by the following theorem.

Theorem 1: Suppose that Assumptions 1 to 3 hold, the guidance system (11) with the represented RPN method (16) admits the following statements:

(i) if the target does not maneuver, the states of the guidance system (11) asymptotically converge to the origin;

(ii) if the target does maneuver, the states of the guidance system (11) asymptotically converge to a neighborhood of the origin.

Proof: Define $\boldsymbol{\omega}_L=\lambda_x\boldsymbol{i}_L+\lambda_y\boldsymbol{j}_L+\lambda_z\boldsymbol{k}_L$, from (15) we obtains

$$\boldsymbol{\omega}_R=\lambda_y\boldsymbol{j}_L+\lambda_z\boldsymbol{k}_L \tag{18}$$

Consider the rotation matrix $\boldsymbol{R}_{LOS}^M=\mathcal{R}_z(\theta_m)\mathcal{R}_y(\psi_m)$, which rotates the LOS frame to the interceptor missile frame. The matrix $\mathcal{R}_a(b)$ indicates that rotation of b along the axis a. The angular rates vector $\boldsymbol{\omega}_R|_M$ in the interceptor missile frame can be deduced as

$$\begin{aligned}\boldsymbol{\omega}_R|_M&=\boldsymbol{R}_{LOS}^M\cdot\boldsymbol{\omega}_R\\&=\left(\sin\theta_m\lambda_y-\cos\theta_m\sin\psi_m\lambda_z\right)\boldsymbol{i}_M\\&\quad+\left(\cos\theta_m\lambda_y+\sin\theta_m\sin\psi_m\lambda_z\right)\boldsymbol{j}_M+\cos\theta_m\lambda_z\boldsymbol{k}_M\end{aligned} \tag{19}$$

Then, the represented RPN guidance law (16) can be expressed in the interceptor missile frame as

$$\begin{aligned}a_{ym}&=N_RV_m\cos\psi_m\lambda_z\\a_{zm}&=-N_RV_m\left(\cos\theta_m\lambda_y+\sin\theta_m\sin\psi_m\lambda_z\right)\end{aligned} \tag{20}$$

If N_R is chosen such that equality (17) valid, then substituting the guidance commands (20) into the system (11) obtains

$$\begin{aligned}&\begin{bmatrix}\ddot{\theta}_L\\ \ddot{\psi}_L\end{bmatrix}\\&=\boldsymbol{F}+\boldsymbol{D}+\boldsymbol{B}\begin{bmatrix}N_RV_m\cos\psi_m\lambda_z\\ -N_RV_m\left(\cos\theta_m\lambda_y+\sin\theta_m\sin\psi_m\lambda_z\right)\end{bmatrix}\\&=\boldsymbol{F}+\boldsymbol{D}+\begin{bmatrix}\frac{N\dot{r}\dot{\theta}_L}{r}\\ \frac{N\dot{r}\dot{\theta}_L\cos\theta_L}{r\cos\theta_L}\end{bmatrix}\end{aligned} \tag{21}$$

Define $\boldsymbol{X}=[\dot{\theta}_L,\dot{\psi}_L\cos\theta_L]^T$. Consider a Lyapunov function candidate as follows.

$$V=\frac{1}{2}\boldsymbol{X}^T\boldsymbol{X} \tag{22}$$

Differentiating the Lyapunov function (22) along the system (21) with respect to time results in

$$\begin{aligned}\dot{V}&=\boldsymbol{X}^T\dot{\boldsymbol{X}}=\boldsymbol{X}^T\begin{bmatrix}\ddot{\theta}_L\\ \ddot{\psi}_L\cos\theta_L-\dot{\psi}_L\dot{\theta}_L\sin\theta_L\end{bmatrix}\\&=\boldsymbol{X}^T\begin{bmatrix}f_1+d_1+\frac{N\dot{r}}{r}\dot{\theta}_L\\ \left(f_2+d_2+\frac{N\dot{r}}{r}\dot{\psi}_L\right)\cos\theta_L+-\dot{\psi}_L\dot{\theta}_L\sin\theta_L\end{bmatrix}\\&\leq-\frac{(N-2)\,|\dot{r}|}{r}\boldsymbol{X}^T\boldsymbol{X}+\|\boldsymbol{X}\|\,\|\boldsymbol{D}\|\\&\leq-\frac{2\,(N-2)\,|\dot{r}|}{r}V+\|\boldsymbol{X}\|\,\|\boldsymbol{D}\|\end{aligned} \tag{23}$$

If the target does not maneuver, (23) can be simplified as

$$\dot{V} \leq -\frac{2\,(N-2)\,|\dot{r}|}{r}V \leq -\frac{2\,(N-2)\,|\dot{r}|_{\min}}{r_0}V \tag{24}$$

where $|\dot{r}|_{\min}$ is the smallest relative speed, r_0 is the initial relative range. From (24) we can conclude that statement (i) is valid.

If the target does maneuver, based on Assumption 1 to 2, there exist a positive real number, $L > 0$, so that $\|\boldsymbol{D}\| \leq L$ holds. Then, (23) can be derived as

$$\begin{aligned}\dot{V} &\leq -\frac{(N-2)\,|\dot{r}|}{r}V + \|\boldsymbol{X}\|\left(\|\boldsymbol{D}\| - \frac{(N-2)\,|\dot{r}|}{2r}\|\boldsymbol{X}\|\right)\\ &\leq -\frac{(N-2)\,|\dot{r}|}{r}V + \|\boldsymbol{X}\|\left(L - \frac{(N-2)\,|\dot{r}|}{2r}\|\boldsymbol{X}\|\right)\end{aligned} \tag{25}$$

Based on (25), it can be concluded that the states of system (11) asymptotically converge to a neighborhood of the origin. The neighborhood is defined as:

$$\mathcal{D} = \left\{\dot{\theta} \in \mathbf{R}, \dot{\psi} \in \mathbf{R} \middle| \|\boldsymbol{X}\| \leq \frac{2rL}{(N-2)\,|\dot{r}|}\right\}$$

Hence, the statement (ii) is valid.

The proof is completed.

Remark 1: The RPN guidance law in [6], [7] is proposed based on geometrical analysis accounting for the multi-value property of the collision triangle. The represented RPN guidance law of this paper is deduced based on the control theory, where a completed Lyapunov analysis is performed. The counter-intuitive negative proportional gain is proven to be regular control parameters design.

The represented RPN guidance law can be directly applied based on the proposed relative dynamics. However, the RPN method does not robust to the maneuvers of a target. Thus, we will introduce the SMC approach to obtain 3D robust HP guidance law.

B. SMC BASED 3D ROBUST HP GUIDANCE LAW

To nullify the LOS angular rate within finite time, the SMC method is introduced to design the 3D robust HP guidance law. The following sliding mode surface is selected:

$$\boldsymbol{S} = \begin{bmatrix} s_1 \\ s_2 \end{bmatrix} = \begin{bmatrix} \dot{\theta}_L \\ \dot{\psi}_L \end{bmatrix} \tag{26}$$

The derivative of $\boldsymbol{S}$ can be deduced from (11).

$$\dot{\boldsymbol{S}} = \begin{bmatrix} \ddot{\theta}_L \\ \ddot{\psi}_L \end{bmatrix} = \boldsymbol{F} + \boldsymbol{D} + \boldsymbol{B}\boldsymbol{u} \tag{27}$$

Then the guidance law is designed as:

$$\boldsymbol{u} = -\boldsymbol{B}^{-1}\left(\boldsymbol{F} + k\lceil\boldsymbol{S}\rfloor^{\alpha} + \boldsymbol{H}\lceil\boldsymbol{S}\rfloor^{0}\right) \tag{28}$$

where $\boldsymbol{H} = diag\{h_1, h_2\}$, $0 < \alpha < 1$, and k, h_1, and h_2 are positive constants, $h = \min\{h_1, h_2\}$ is chosen such that $h \geq \|\boldsymbol{D}\|$.

Theorem 2: Consider system (11), and suppose that the Assumption 1 to 3 hold. If choose (26) as the sliding surface, and (28) as the guidance law, then the states of system (11) will converge to the origin within a finite time.

Proof: Consider a Lyapunov function candidate as (29)

$$V = \frac{1}{2}\boldsymbol{S}^T\boldsymbol{S} \tag{29}$$

Taking derivative of the sliding surface (27) into account, the time derivative of V results in

$$\begin{aligned}\dot{V} &= \boldsymbol{S}^T\dot{\boldsymbol{S}}\\ &= \boldsymbol{S}^T\left(\boldsymbol{F} + \boldsymbol{D} + \boldsymbol{B}\boldsymbol{u}\right)\\ &= \boldsymbol{S}^T\left(\boldsymbol{D} - k\lceil\boldsymbol{S}\rfloor^{\alpha} - \boldsymbol{H}\lceil\boldsymbol{S}\rfloor^{0}\right)\\ &\leq -k\boldsymbol{S}^T\lceil\boldsymbol{S}\rfloor^{\alpha} - (|s_1| + |s_2|)\,(h - \|\boldsymbol{D}\|)\end{aligned} \tag{30}$$

Since h is chosen such that $h \geq \|D\|$ holds, $h - \|\boldsymbol{D}\| \geq 0$ is positive definite. Moreover, according to Lemma 2 and the sliding surface (26), the term $\boldsymbol{S}^T\lceil\boldsymbol{S}\rfloor^{\alpha}$ can be expressed as

$$\boldsymbol{S}^T\lceil\boldsymbol{S}\rfloor^{\alpha} = |s_1|^{1+\alpha} + |s_2|^{1+\alpha} \geq \left(|s_1|^2 + |s_2|^2\right)^{\frac{1+\alpha}{2}} \tag{31}$$

Then the derivative of the Lyapunov function can be further deduced as

$$\dot{V} \leq -\frac{k}{2^{(1+\alpha)/2}}V^{(1+\alpha)/2} \tag{32}$$

According to Lemma 1, it can be concluded that the states of the system (11) will converge to zero within finite time T.

$$T \leq \frac{2^{1+\alpha/2}}{k\,(1-\alpha)}V^{(1-\alpha)/2}(\boldsymbol{S}_0) \tag{33}$$

where $\boldsymbol{S}_0$ is the initial state vector of the sliding surface, and the initial time is assumed to be zero.

Since the sliding variables equal to the states of the guidance system (11), it can be concluded that the system states converge to zero within a finite time.

Remark 2: The less-aggressive hit-to-kill strategy [30] can also be used to design the 3D robust HP guidance law. Moreover, the application of the SMC based 3D robust HP guidance law shows the effectiveness of the proposed HP guidance law design framework.

IV. NTSM BASED ANGLE CONSTRAINED GUIDANCE

To track the given LOS angles and to nullify the LOS angular rates, the following state vector is defined.

$$\boldsymbol{x} = \begin{bmatrix} x_1 \\ x_2 \end{bmatrix} = \begin{bmatrix} \theta_L - \theta_L^* \\ \psi_L - \psi_L^* \end{bmatrix} \tag{34}$$

where, the desired LOS angles, θ_L^* and ψ_L^* are assumed to be constants. Based on (34), the nominal model (11) can be expressed as

$$\ddot{\boldsymbol{x}} = \begin{bmatrix} \ddot{x}_1 \\ \ddot{x}_2 \end{bmatrix} = \begin{bmatrix} \ddot{\theta}_L \\ \ddot{\psi}_L \end{bmatrix} = \boldsymbol{F} + \boldsymbol{D} + \boldsymbol{B}\boldsymbol{u} \tag{35}$$

Then the following nonsingular terminal sliding surface is selected [25]:

$$\boldsymbol{S} = \begin{bmatrix} s_1 & s_2 \end{bmatrix}^T = \boldsymbol{x} + \beta \lceil \dot{\boldsymbol{x}} \rfloor^{\alpha} \tag{36}$$

where $1 < \alpha < 2$ and $\beta > 0$.

Based on the definition of the new state $\boldsymbol{x}$, the derivative of the sliding surface can be deduced as

$$\begin{aligned} \dot{\boldsymbol{S}} &= \dot{\boldsymbol{x}} + \alpha\beta \begin{bmatrix} |\dot{x}_1|^{\alpha-1} & 0 \\ 0 & |\dot{x}_2|^{\alpha-1} \end{bmatrix} \begin{bmatrix} \ddot{x}_1 \\ \ddot{x}_2 \end{bmatrix} \\ &= \alpha\beta \boldsymbol{G} \left(\frac{1}{\alpha\beta} \lceil \dot{\boldsymbol{x}} \rfloor^{2-\alpha} + \boldsymbol{F} + \boldsymbol{D} + \boldsymbol{B}\boldsymbol{u} \right) \end{aligned} \tag{37}$$

where $\boldsymbol{G} = diag\left\{ |\dot{x}_1|^{\alpha-1}, |\dot{x}_2|^{\alpha-1} \right\}$. Based on the equivalent control approach, the following guidance law is proposed.

$$u = -\boldsymbol{B} \left(\boldsymbol{F} + \frac{1}{\alpha\beta} \lceil \dot{\boldsymbol{x}} \rfloor^{2-\alpha} + \lceil \boldsymbol{S} \rfloor^{\gamma} + \boldsymbol{H} \lceil \boldsymbol{S} \rfloor^{0} \right) \tag{38}$$

where $\lceil \boldsymbol{S} \rfloor^{\gamma}$ denotes the lower power reaching law, and $0 < \gamma < 1$. $\boldsymbol{H} = diag\{h_1, h_2\}$ the gain of the discontinuous control term. $h_1, h_2 > 0$, $h = \min\{h_1, h_2\}$ is chosen such that $h \geq \|\boldsymbol{D}\|$. Then the stability of the LOS angle constrained guidance system is summarized as follows.

Theorem 3: Consider the system (34) and (35). Suppose the Assumption 1 to 3 hold. if taking (36) as the sliding surface, (38) as the control law, the following statements can be achieved.

(i) $\boldsymbol{S} = 0$ is reached within a finite time;

(ii) the states of the system (34) and (35) converge to zero within a finite time.

Proof: Consider the following Lyapunov candidate.

$$V = \frac{1}{2} \boldsymbol{S}^T \boldsymbol{S} \tag{39}$$

The time derivative of the Lyapunov function V can be deduced as

$$\begin{aligned} \dot{V} &= \boldsymbol{S}^T \dot{\boldsymbol{S}} \\ &= \boldsymbol{S}^T \alpha\beta \boldsymbol{G} \left(\frac{1}{\alpha\beta} \lceil \dot{\boldsymbol{x}} \rfloor^{2-\alpha} + \boldsymbol{F} + \boldsymbol{D} + \boldsymbol{B}\boldsymbol{u} \right) \\ &= \boldsymbol{S}^T \alpha\beta \boldsymbol{G} \left(\boldsymbol{D} - \lceil \boldsymbol{S} \rfloor^{\gamma} - \boldsymbol{H} \lceil \boldsymbol{S} \rfloor^{0} \right) \end{aligned} \tag{40}$$

After some algebraic manipulations, we get

$$\begin{aligned} \dot{V} = &-\alpha\beta \begin{bmatrix} |\dot{x}_1|^{\alpha-1} & 0 \\ 0 & |\dot{x}_2|^{\alpha-1} \end{bmatrix} \begin{bmatrix} |s_1|^{1+\gamma} \\ |s_2|^{1+\gamma} \end{bmatrix} \\ &-\alpha\beta \begin{bmatrix} (h_1 - d_1) |\dot{x}_1|^{\alpha-1} |s_1| \\ (h_2 - d_2) |\dot{x}_2|^{\alpha-1} |s_2| \end{bmatrix} \end{aligned} \tag{41}$$

As discussed in [24], [25], $\dot{x}_i = 0$ is just a transient state unless $s_i = 0$ is achieved, where $i = 1, 2$. Therefore, let

$$\dot{x}_{\min} \triangleq \min\{\dot{x}_1, \dot{x}_2\}$$

where $\dot{x}_1 \neq 0$ and $\dot{x}_2 \neq 0$. Moreover, since $h > \|\boldsymbol{D}\|$ is valid, (41) can be further deduced as

$$\begin{aligned} \dot{V} &\leq -\alpha\beta\dot{x}_{\min} \begin{bmatrix} |s_1|^{1+\gamma} \\ |s_2|^{1+\gamma} \end{bmatrix} - \alpha\beta\dot{x}_{\min} \begin{bmatrix} (h_1 - d_1) |s_1| \\ (h_2 - d_2) |s_2| \end{bmatrix} \\ &\leq -\alpha\beta\dot{x}_{\min} 2^{\frac{1+\gamma}{2}} V^{\frac{1+\gamma}{2}} - \alpha\beta\dot{x}_{\min} (h - \|D\|) V^{\frac{1}{2}} \\ &\leq -\alpha\beta\dot{x}_{\min} 2^{\frac{1+\gamma}{2}} V^{\frac{1+\gamma}{2}} \end{aligned} \tag{42}$$

According to Lemma 1, for the case of $\dot{x}_1 \neq 0$ and $\dot{x}_2 \neq 0$, the inequality (42) indicates that the sliding surface will be reached within a finite time. Except for the case that $s_i = 0$ is achieved, the crossing process of $\dot{x}_i = 0$ will be completed within finite time as shown in [25]. Therefore, the states of the system will reach the sliding mode $\boldsymbol{S} = 0$ within a finite time. The proof of the statement (i) has been completed.

After the system states reach the sliding surface, the following equality is valid.

$$x_i + \beta \lceil \dot{x}_i \rfloor^{\alpha} = 0, \quad i = 1, 2 \tag{43}$$

Consider the following Lyapunov function candidate

$$V_i = \tfrac{1}{2} x_i x_i, \quad for\ i = 1, 2 \tag{44}$$

Differentiating the Lyapunov function (44) obtains

$$\dot{V}_i = x_i \dot{x}_i = x_i \lceil \frac{-1}{\beta} x_i \rfloor^{\frac{1}{\alpha}} = -\frac{1}{\beta^{\frac{1}{\alpha}}} |x_i|^{\frac{1+\alpha}{\alpha}} = -\frac{2^{\frac{1+\alpha}{2\alpha}}}{\beta^{\frac{1}{\alpha}}} V_i^{\frac{1+\alpha}{2\alpha}} \tag{45}$$

According to Lemma 1 and the equality (43), the states of the system (34) and (35) converge to zero within a finite time. The proof of the statement (ii) is completed.

Remark 3: As in many literatures, the angle constraints can be transformed to be LOS angle constraints [17]–[24]. The proposed LOS angle constrained guidance law shows the feasibility of the presented HP guidance design framework. Moreover, according to the relationship between the two LOS reference frame, (7) and (8), the convergence of x and $\dot{x}$ indicate that

$$\theta_{L,M} \to -\theta_L^*, \quad \psi_{L,M} \to \psi_L^* - \pi, \quad \dot{\theta}_{L,M} = \dot{\psi}_{L,M} = 0$$

TABLE 1. Units for magnetic properties.

Items	Initial Parameters ($\tau = 0$)
Interceptor	$(x_M, y_M, z_M) = (18, 9.6, 2) \times 10^3$ m , $V_m = 1500$ m/s
	$\theta_M = -8^\circ$, $\psi_M = -175^\circ$, for HO interception
	$\theta_M = -1^\circ$, $\psi_M = -5^\circ$, for HP interception
	$\lvert a_{ym}(\tau) \rvert \leq 10 \cdot g$, $\lvert a_{zm}(\tau) \rvert \leq 10 \cdot g$
Target	$(x_T, y_T, z_T) = (100, 10000, 0)$ m , $V_t = 2100$ m/s
	$\theta_T = -1^\circ$, $\psi_T = -5^\circ$, $a_{yt}(\tau) = a_{zt}(\tau) = 0$ or
	$a_{yt}(\tau) = -3g \cdot \sin(\tau/2)$, $a_{zt}(\tau) = 3g \cdot \mathrm{sign}(\sin(\tau/2))$

V. NUMERICAL SIMULATION

This section illustrates the feasibility of the proposed robust HP guidance laws. The engagement scenario is organized as in Table 1, where τ is the time moment and $g = 9.81\text{m/s}^2$ is the gravity acceleration. The simulation step is set to be

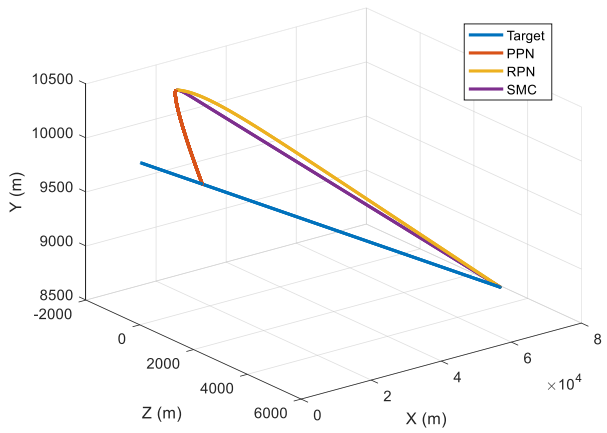

(a) Three-dimensional trajectory

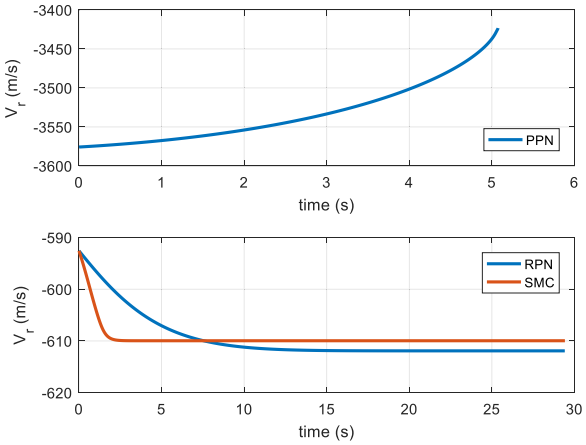

(b) Relative velocity

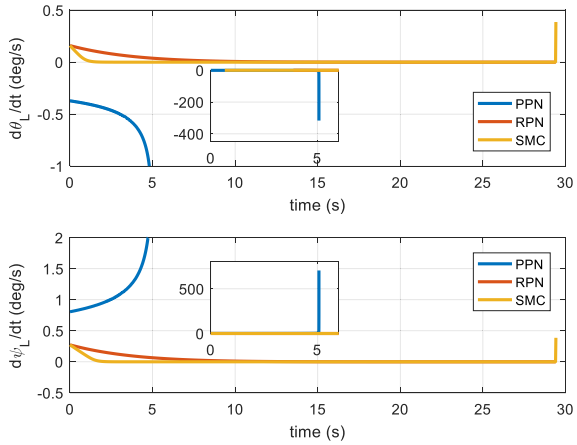

(c) LOS angular rates

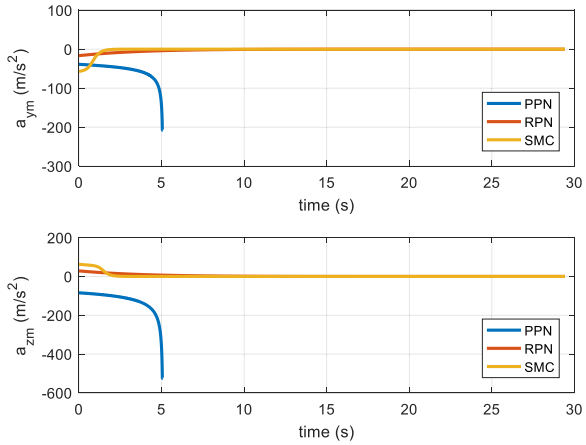

(d) Lateral accelerations of the interceptor missile

FIGURE 2. Simulation results for intercepting a non-maneuvering target.

1 ms. The dynamics of the interceptor missile and the target is integrated via the 4th-order Runge-Kutta method. The seeker is assumed to be effective when $r > 100$m, otherwise, the interceptor missile will perform the last valid guidance command to the end of the engagement.

A. CASE OF HIT-TO-KILL INTERCEPTION

In this part, the guidance laws based on the concept of nullifying the LOS angular rates will be verified. Except for the proposed RPN guidance law (16) and the SMC based guidance law (28), the traditional PPN guidance law is used for comparison. The PPN guidance law takes the form of

$$\boldsymbol{u} = N\boldsymbol{\omega}_{R,M} \times \boldsymbol{V}_M \tag{46}$$

where $N = 4$. $\boldsymbol{\omega}_{R,M} = \dot{\psi}_{L,M}\cos\theta_{L,M}\boldsymbol{j}_{L,M} + \dot{\theta}_{L,M}\boldsymbol{k}_{L,M}$, where $\boldsymbol{j}_{L,M}$ and $\boldsymbol{k}_{L,M}$ are the unit vectors of axis y and z of the LOS-M. According to (7) and (8), the necessary variables in $\boldsymbol{\omega}_{R,M}$ can be obtained by the following equalities.

$$\theta_{L,M} = -\theta_L, \quad \dot{\theta}_{L,M} = \dot{\theta}_L, \quad \dot{\psi}_{L,M} = \dot{\psi}_L$$

Then the LOS angular rate vector $\boldsymbol{\omega}_{R,M}$ can be rotated to the interceptor missile's frame based on the rotation matrix

$$\boldsymbol{R}^M_{LOS-M} = \mathcal{R}_z(\theta_m)\,\mathcal{R}_y(\psi_m - \pi)$$

The parameter N_R of the RPN guidance law is set to be $N_R = -4$. In the SMC based guidance law (28), $k = 10$, $\alpha = 0.5$, $h_1 = h_2 = 50$. Moreover, the hyperbolic tangent function is employed to replace the signum function such that the chattering phenomenon is cancelled [31].

$$\tanh\left(\frac{x}{\varepsilon}\right) = \frac{e^{x/\varepsilon} - e^{-x/\varepsilon}}{e^{x/\varepsilon} + e^{-x/\varepsilon}}, \quad x \in \mathbf{R}, \quad \varepsilon \in \mathbf{R}_+ \tag{47}$$

where $\varepsilon = 0.05$°/s. The simulation results are shown as in Figure 2, Figure 3, and Table 2.

Table 2 directly shows that the HP guidance methods admit better interception accuracy in the price of longer engagement time. In the interception engagement that using a speed inferior interceptor missile to intercept a speed superior target, both of the HO interception mode and the HP interception mode can be chosen. However, the relative velocity in the HO

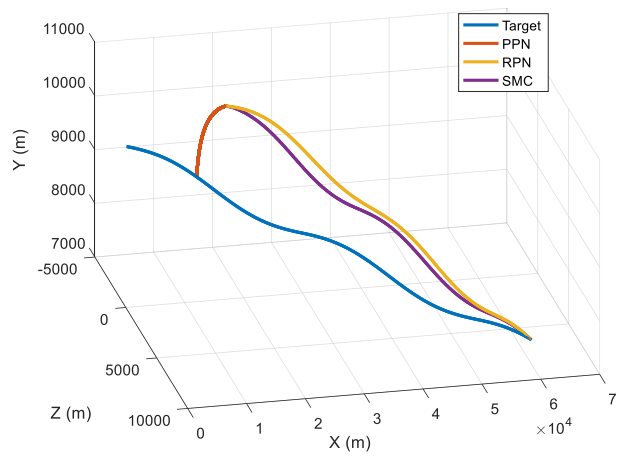

(a) Three-dimensional trajectory

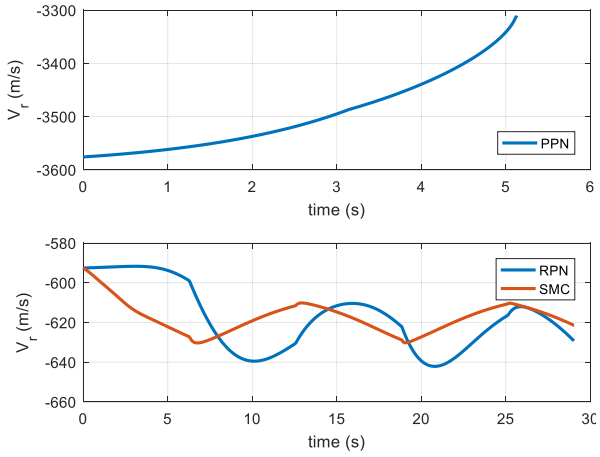

(b) Relative velocity

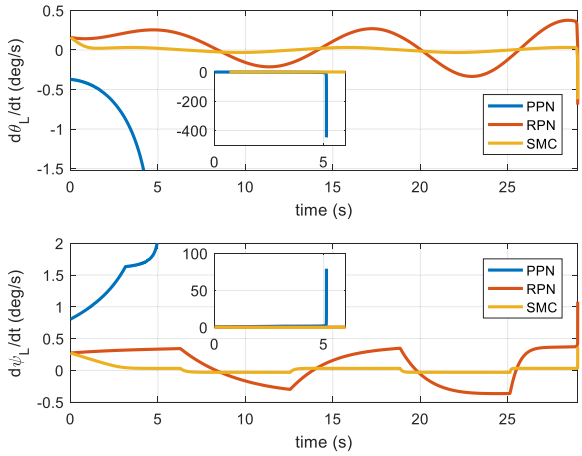

(c) LOS angular rates

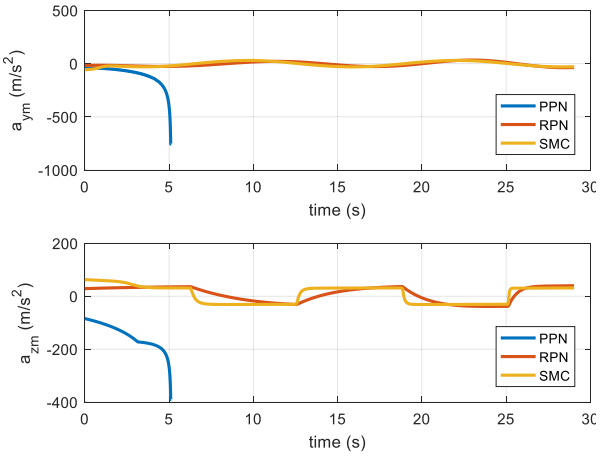

(d) Lateral accelerations of the interceptor missile

FIGURE 3. Simulation results for intercepting a maneuvering target.

TABLE 2. Performances of different guidance laws.

Guidance law	Target maneuver	Terminal range (m)	Ending time (s)
PPN	No	2.149	5.076
RPN		0.4095	29.416
SMC		0.1166	29.422
PPN	Yes	1.254	5.128
RPN		0.4687	29.032
SMC		0.2020	29.039

interception mode is much bigger than that in the HP interception mode (see the subgraphs b in Figure 2 and in Figure 3).

This situation results in stringent requirements on the guidance and control systems of the interceptor missile. In addition, although the PN methods are not robust to the target maneuver, the RPN approach achieves better guidance performance with smaller control efforts than that of the PPN method (see the subgraphs c and d in Figure 3). The SMC based guidance law exhibits high guidance accuracy and robustness to the target maneuver. The utilization of hyperbolic tangent function cancels the chattering effect (see subgraph c in Figure 3).

B. CASE OF ANGLE CONSTRAINED INTERCEPTION

In this part, the LOS angle constrained NTSM guidance law (38) will be verified. The parameters of the guidance law are set as $\alpha = 1.2$, $\beta = 8.0$, $\gamma = 0.5$, and $h_1 = h_2 = 0.5$. The hyperbolic tangent function (47) is also used to replace the signum function with $\varepsilon = \pi/180$. The desired LOS angles and the performances of the guidance law are listed in Table 3. The graphic simulation results can be found in Figure 4.

In the simulations, a maneuvering target is considered. According to Table 3, the proposed NTSM guidance law leads the interceptor missile successfully intercept the target with the desired LOS angles. Taking the subgraph (e) in Figure 4 into account, the proposed guidance law ensures that the states of the guidance system reach the sliding surface within finite time. Then, the LOS angles and the LOS angular rates converge to the equilibrium within a finite time (see subgraphs (c) and (d) in Figure 4).

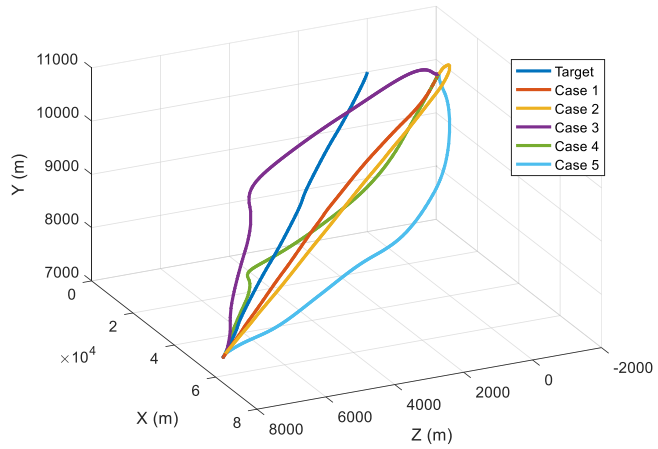

(a) Three-dimensional trajectory

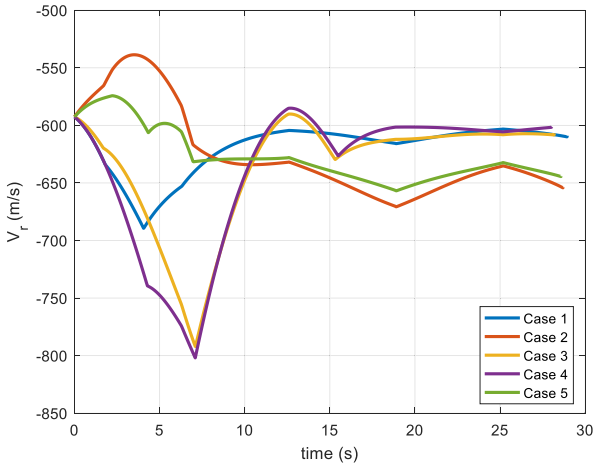

(b) Relative velocity

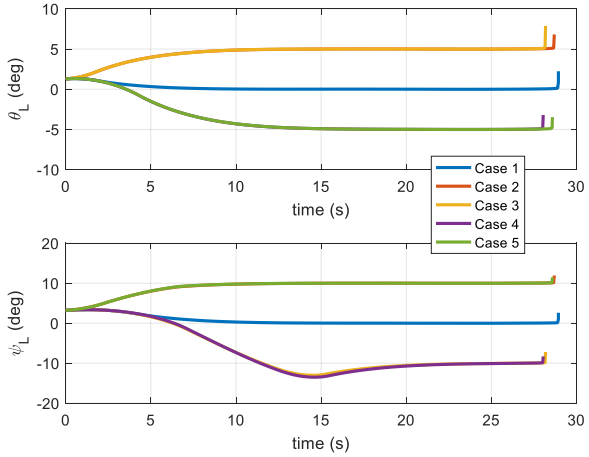

(c) The LOS angles of the interceptor missile

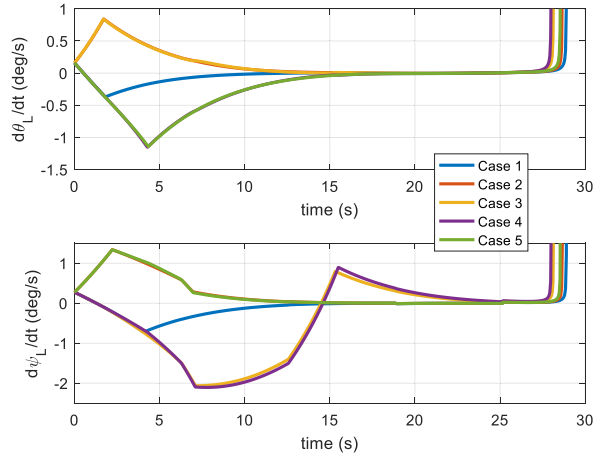

(d) The LOS angles of the interceptor missile

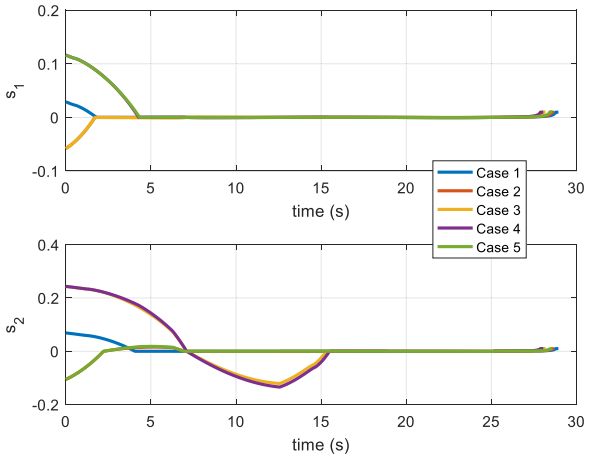

(e) The sliding surfaces

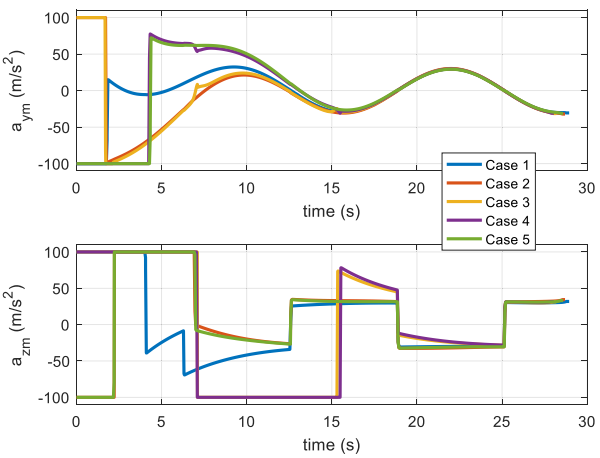

(f) Lateral accelerations of the interceptor missile

FIGURE 4. **Simulation results of LOS angle constrained NTSM guidance law.**

In addition, since the control effort in the elevation direction affects the dynamics in the azimuth direction, the convergence process of the LOS angle and LOS angular rate in the azimuth is longer than that in the elevation. From the curves of the lateral guidance accelerations, as shown in subgraph (f) of Figure 4, the lateral acceleration $a_{zm}(t)$ needs more time to converge to the necessary level. Moreover, comparing the desired LOS angles in Table 3 and the three-dimensional

TABLE 3. The desired LOS angles and the performances.

Case number	Desired LOS angle (°)	Terminal range (m)	Ending time (s)
1	$\theta_{Lf}^{*}=0^{\circ},\psi_{Lf}^{*}=0^{\circ}$	0.2792	28.943
2	$\theta_{Lf}^{*}=5^{\circ},\psi_{Lf}^{*}=10^{\circ}$	0.3374	28.701
3	$\theta_{Lf}^{*}=5^{\circ},\psi_{Lf}^{*}=-10^{\circ}$	0.3097	28.189
4	$\theta_{Lf}^{*}=-5^{\circ},\psi_{Lf}^{*}=-10^{\circ}$	0.1887	28.051
5	$\theta_{Lf}^{*}=-5^{\circ},\psi_{Lf}^{*}=10^{\circ}$	0.2251	28.590

trajectories in the subgraphs (a) and (c) of Figure 4. The bigger the initial derivations between the initial LOS angles and the desired ones, the more curled the interceptor missile's trajectories are. Meanwhile, the convergence time of the sliding variable is increased along with the growth of the initial LOS angles derivation.

VI. CONCLUSION

In this paper, a target based HP interception guidance law design framework has been proposed and verified. In view of the relationship of the HP interception mode and the TC interception mode, the HP interception engagement is formulated as a target passively chases after the interceptor missile. Based on the presented model, the RPN guidance law is reformulated, where a Lyapunov analysis shows that the RPN guidance law guarantees the asymptotical stability of the guidance system. The completed analysis of SMC based robust HP guidance law demonstrates that the classical robust control methods can be applied to develop 3D robust HP guidance law via the proposed design framework. At the last, the successful application of the NTSM based guidance law shows another approach for angle constrained HP guidance law design.

REFERENCES

[1] O. Golan and T. Shima, "Head pursuit guidance for hypervelocity interception," presented at the AIAA Guid., Navigat., Control Conf. Exhibit, Providence, RI, USA, 2004.

[2] G. Lianzheng, S. Yi, G. Yunfeng, and Z. Lijun, "Head pursuit variable structure guidance law for three-dimensional space interception," *Chin. J. Aeronaut.*, vol. 21, no. 3, pp. 247–251, Jun. 2008.

[3] T. Shima, "Deviated velocity pursuit," presented at the AIAA Guid., Navigat. Control Conf. Exhibit, 2007.

[4] T. Shima and O. M. Golan, "Head pursuit guidance," *J. Guid., Control, Dyn.*, vol. 30, no. 5, pp. 1437–1444, Sep. 2007.

[5] C. Zhang, K. Zhang, and J. Wang, "An adaptive terminal sliding mode guidance law for head pursuit interception with impact angle considered," in *Proc. Inform. Control, Autom. Robot., 13th Int. Conf. (ICINCO)*, K. Madani, D. Peaucelle, and O. Gusikhin, Eds. Cham, Switzerland: Springer, 2018, pp. 277–292.

[6] H. M. Prasanna and D. Ghose, "Retro-Proportional-navigation: A new guidance law for interception of high speed targets," *J. Guid., Control, Dyn.*, vol. 35, no. 2, pp. 377–386, Mar. 2012.

[7] S. Ghosh, D. Ghose, and S. Raha, "Three dimensional retro-PN based impact time control for higher speed nonmaneuvering targets," in *Proc. 52nd IEEE Conf. Decis. Control*, Dec. 2013, pp. 4865–4870.

[8] S. Nath and D. Ghose, "Path length constrained interception of higher speed targets using retro-proportional navigation guidance law," in *Proc. AIAA Scitech Forum*, Jan. 2020, p. 0611.

[9] P. Zarchan, *Tactical and Strategic Missile Guidance*, 6th ed. Reston, VA, USA: American Institute of Aeronautics and Astronautics, 2012.

[10] T. Shima, "Intercept-angle guidance," *J. Guid., Control, Dyn.*, vol. 34, no. 2, pp. 484–492, Mar. 2011.

[11] S. Sun, D. Zhou, J. Zhou, and K. L. Teo, "A generalized design method for three-dimensional guidance laws," *Proc. Inst. Mech. Eng., G, J. Aerosp. Eng.*, vol. 231, no. 1, pp. 47–60, Jan. 2017.

[12] G. Li and H. Ji, "A three-dimensional robust nonlinear terminal guidance law with ISS finite-time convergence," *Int. J. Control*, vol. 89, no. 5, pp. 938–949, May 2016.

[13] G. Li, M. Xin, and C. Miao, "Finite-time input-to-state stability guidance law," *J. Guid., Control, Dyn.*, vol. 41, no. 10, pp. 2199–2213, Oct. 2018.

[14] J. Guo, Y. Li, and J. Zhou, "A new continuous adaptive finite time guidance law against highly maneuvering targets," *Aerosp. Sci. Technol.*, vol. 85, pp. 40–47, Feb. 2019.

[15] J. Guo, Y. Li, and J. Zhou, "An observer-based continuous adaptive sliding mode guidance against chattering for homing missiles," *Trans. Inst. Meas. Control*, vol. 41, no. 12, pp. 3309–3320, Aug. 2019.

[16] R. V. Nanavati, S. R. Kumar, and A. Maity, "Lead-angle-based three-dimensional guidance for angle-constrained interception," *J. Guid., Control, Dyn.*, vol. 44, no. 1, pp. 190–199, 2020.

[17] A. Ratnoo, "Analysis of two-stage proportional navigation with heading constraints," *J. Guid., Control, Dyn.*, vol. 39, no. 1, pp. 156–164, Jan. 2016.

[18] V. Hirwani and A. Ratnoo, "Field-of-view constrained polynomial guidance law for interception of moving target using dual-seeker interceptors," *IFAC-PapersOnLine*, vol. 51, no. 1, pp. 377–382, 2018.

[19] B. Liu, M. Hou, Y. Yu, and Z. Wu, "Three-dimensional impact angle control guidance with field-of-view constraint," *Aerosp. Sci. Technol.*, vol. 105, Oct. 2020, Art. no. 106014.

[20] Y. Liao, H. Li, and W. Bao, "Three-dimensional diving guidance for hypersonic gliding vehicle via integrated design of FTNDO and AMSTSMC," *IEEE Trans. Ind. Electron.*, vol. 65, no. 3, pp. 2704–2715, Mar. 2018.

[21] B. Biswas, A. Maity, and S. R. Kumar, "Finite-time convergent three-dimensional nonlinear intercept angle guidance," *J. Guid., Control, Dyn.*, vol. 43, no. 1, pp. 146–153, Jan. 2020.

[22] Y. Tian, Y. Cai, Z. Yu, and Y. Deng, "Three-dimensional fast fixed-time convergence guidance law with impact angle constraint," *IEEE Access*, vol. 7, pp. 180467–180481, 2019.

[23] Y. Si and S. Song, "Adaptive reaching law based three-dimensional finite-time guidance law against maneuvering targets with input saturation," *Aerosp. Sci. Technol.*, vol. 70, pp. 198–210, Nov. 2017.

[24] S. R. Kumar and D. Ghose, "Three-dimensional impact angle guidance with coupled engagement dynamics," *Proc. Inst. Mech. Eng., G, J. Aerosp. Eng.*, vol. 231, no. 4, pp. 621–641, Mar. 2017.

[25] Y. Feng, X. Yu, and Z. Man, "Non-singular terminal sliding mode control of rigid manipulators," *Automatica*, vol. 38, no. 12, pp. 2159–2167, Dec. 2002.

[26] S.-H. Song and I.-J. Ha, "A Lyapunov-like approach to performance analysis of 3-dimensional pure PNG laws," *IEEE Trans. Aerosp. Electron. Syst.*, vol. 30, no. 1, pp. 238–248, Jan. 1994.

[27] A. Polyakov and L. Fridman, "Stability notions and Lyapunov functions for sliding mode control systems," *J. Franklin Inst.*, vol. 351, no. 4, pp. 1831–1865, Apr. 2014.

[28] H. Hardy, J. E. Littlewood, and G. Polya, *Inequalities*, 2nd ed. Cambridge, U.K.: Cambridge Univ. Press, 1952.

[29] K.-B. Li, H.-S. Shin, A. Tsourdos, and M.-J. Tahk, "Capturability of 3D PPN against lower-speed maneuvering target for homing phase," *IEEE Trans. Aerosp. Electron. Syst.*, vol. 56, no. 1, pp. 711–722, Feb. 2020.

[30] B. Kada, "Arbitrary-order sliding-mode-based homing-missile guidance for intercepting highly maneuverable targets," *J. Guid., Control, Dyn.*, vol. 37, no. 6, pp. 1999–2013, Nov. 2014.

[31] D. Zhou and B. Xu, "Adaptive dynamic surface guidance law with input saturation constraint and autopilot dynamics," *J. Guid., Control, Dyn.*, vol. 39, no. 5, pp. 1155–1162, May 2016.

FENG YANG was born in Baoji, Shanxi, China, in 1987. He received the B.S. degree in flight vehicle design and engineering, and the M.S. and Ph.D. degrees in flight vehicle design from the Harbin Institute of Technology, Harbin, China, in 2009, 2011, and 2019, respectively.

Since 2019, he has been working with the Postdoctoral Program of Mechanical, School of Aeronautics and Astronautics, Dalian University of Technology, Dalian, China. His research interests include advanced guidance and control methods of flight vehicle, sliding mode control theory and application, and active disturbance rejection control and application.

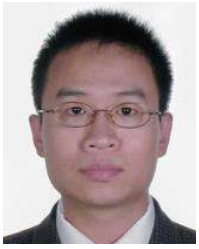

GUANG-QING XIA was born in Shijiazhuang, Hebei, China, in 1979. He received the B.S. degree in flight vehicle propulsion engineering from Northwestern Polytechnical University, Xi'an, China, in 2002, and the M.S. and Ph.D. degrees in aerospace propulsion theory and engineering from Northwestern Polytechnical University in 2005 and 2009.

From 2007 to 2008, he studied with Université Joseph Fourier, as a joint Ph.D. Student, Grenoble, France. From 2009 to 2012, he was a Lecturer with the School of Aeronautics and Astronautics, Dalian University of Technology. He was promoted to be an Associate Professor, in December 2012, and to be a Professor, in December 2017. Since 2018, he has been the Dean of the School of Aeronautics and Astronautics, Dalian University of Technology. Since 2019, he has been the Vice Dean of the State Key Laboratory of Structural Analysis for Industrial Equipment, Dalian University of Technology. He is currently the author of more than 100 articles and more than 20 patents. His research interests include aerospace propulsion technology, micro-nano satellite engineering, and the advanced guidance and control technology.

KAI LIU was born in Yanbian, Jilin, China, in 1984. He received the B.S. degree in computational mathematics from Jilin University, China, in 2007, and the Ph.D. degree in control science and engineering from the Harbin Institute of Technology, China, in 2013.

From 2013 to 2017, he was a Senior Engineer with the Beijing Institute of Technology, Beijing, China. Since 2017, he has been an Associate Professor with the Dalian University of Technology, China. His research interests include guidance, navigation, and control.